Available online at www.sciencedirect.com
ScienceDirect
Journal of Photochemistry and Photobiology A: Chemistry 194 (2008) 20–26
Journal of Photochemistry and Photobiology A:Chemistry
www.elsevier.com/locate/jphotochem

A new ionic liquid based quasi-solid state electrolyte for dye-sensitized solar cells

Miao Wang [a,b], Xong Yin [a,b], Xu Rui Xiao [a], XiaoWen Zhou [a], Zheng Zhong Yang [a], Xue Ping Li [a], Yuan Lin [a,*]

[a] *Beijing National Laboratory for Molecular Sciences, Key Laboratory of Photochemistry, Institute of Chemistry, Chinese Academy of Sciences, Beijing 100080, China*
[b] *Graduate School of Chinese Academy of Sciences, Beijing 100039, China*

Received 13 October 2005; received in revised form 25 June 2007; accepted 12 July 2007
Available online 17 July 2007

Abstract

Ionic liquid based quasi-solid state electrolytes were prepared by solidifying the ionic liquid electrolytes containing 1-hexyl-3-methylidazolium iodide (HMImI) or a binary mixture of HMImI and 1-ethyl-3-methylimidazolium tetrafluoroborate ($EMImBF_4$) with an ionic liquid polymer poly (1-oligo (ethylene glycol) methacrylate-3-methylimidazolium chloride) (P(MOEMImCl)), respectively. The improvements of the ionic conductivity and the apparent diffusion coefficient of triiodide are observed in the binary ionic liquid mixture gel electrolyte. The thermal stability of the quasi-solid state electrolytes is determined by thermogravimetric analysis. The ionic liquid based quasi-solid state electrolytes were successfully used to fabricate the dye-sensitized solar cells achieving the conversion efficiency of 6.1% under the light intensity of 100 mW cm^{-2}.

Keywords: Ionic liquids; Ionic liquid polymer; Quasi-solid state electrolytes; Dye-sensitized solar cells; Conversion efficiency

1. Introduction

Dye-sensitized solar cells (DSSCs) with a high conversion efficiency and low cost have been investigated intensively as potential alternative to traditional photovoltaic devices [1–3]. Conversion efficiency of 10% for these nanocrystalline cells was achieved based on the liquid electrolytes containing the organic solvents and the redox species I^-/I_3^-. The major problem of using organic solvent-based electrolytes in DSSCs is the evaporation and leakage of the liquid electrolyte during the long-term operation leading to the decay of the cell performance. For improving the long-term stability, many attempts have been made to substitute the volatile liquid electrolytes with solvent-free solid polymer electrolytes, organic hole transporting materials, etc. [4–8]. Room temperature ionic liquids with the attractive properties of chemical and thermal stability, non-volatility and high ionic conductivity in room temperature were studied extensively for the electrochemical device applications. Various investigations have been carried out to develop the ionic liquid electrolytes as the promising candidate for DSSCs [9–13]. It was reported recently that the conversion efficiency >7% was obtained for the DSSCs with the pure ionic liquid electrolytes [10,14,15]. Furthermore, there are many interests in an attempt to preparing the quasi-solid state electrolytes by solidifying the ionic liquid electrolytes with polymers [16] or nanoparticles [17]. Ionic liquid based quasi solid-state electrolytes having the attractive properties of the ionic liquids are of great advantage for fabrication of high-efficiency DSSCs without evaporation and leakage of the electrolyte during the long-term operation.

In this work, we report a new quasi-solid state electrolyte which was prepared by solidifying the ionic liquid based electrolyte with ionic liquid polymer. Poly (1-oligo (ethylene glycol) methacrylate-3-methylimidazolium chloride) (P(MOEMImCl)) has been synthesized as the ionic liquid polymer [18] exhibiting the higher ionic conductivity about 1.08×10^{-4} S cm^{-1} (25 °C). Additionally, P(MOEMImCl) offers the characteristics of high solubility with the inorganic salts due to the large polarity at the ether oxygen of PEO and good miscibility with the organic

* Corresponding author at: The Chinese Academy of Sciences, N0.2, 1st North Zhongguancun Street, Beijing 100080, PR China. Tel.: +86 10 82615031; fax: +86 10 82617315.
E-mail address: Linyuan@iccas.ac.cn (Y. Lin).

1010-6030/$ – see front matter © 2007 Published by Elsevier B.V.
doi:10.1016/j.jphotochem.2007.07.009

salts in terms of the imidazole group. This is of great advantage for optimization of the organic and inorganic composition of the ionic liquid based quasi-solid state electrolytes achieving the high ionic conductivity and good stability for dye-sensitized solar cells.

2. Experimental

2.1. Materials

Poly (1-oligo(ethylene glycol)methacrylate-3-methylimidazolium chloride) (P(MOEMImCl)) was synthesized according to the literature methods [19,20]. Poly (ethylene glycol) methacrylate (Mw 360, MOE) purchased from SIGMA Co. Ltd. was reacted with thionyl chloride in the presence of pyridine to form MOE-Cl [21]. The product was purified by washing with water. IR spectrum (obtained from Bruker Tensor 27) showed the appearance of a new absorption at 663 cm^{-1} corresponding to the stretching of C–Cl and the absence of the strong absorption of −OH stretching at 3500–3550 cm^{-1} confirming the formation of MOE-Cl. MOE-Cl was dissolved in *N*,*N*-dimethylformamide (DMF) and mixed with an excess of *N*-methylimidazole. The mixture was stirred at 80 °C for 2 days under N_2 atmosphere [22]. The product was purified with dehydrated diethylther and dried at vacuum at 60 °C for 2 days [19]. The structure of MOEMImCl was confirmed by ^1H NMR spectroscopy (Bruker DMX-300) which exhibits the peaks of imidazolium proton at 7.55, 7.69 and 10.10 ppm, respectively. MOEMImCl was polymerized in bulk with azobisisobutyronitrile (AIBN) as the initiator at 60 °C under N_2 atmosphere for 8 h. The obtained polymer P(MOEMImCl) was dried under vacuum at 60 °C for 24 h [23]. Molecular weight of P(MOEMImCl) determined by mass spectrometry (BIFLEXIII MALDI-TOF) is >10,000. The chemical structure of P(MOEMImCl) is shown in Scheme 1.

Ionic liquids of 1-hexyl-3-methylidazolium iodide (HMImI) and 1-ethyl-3-methylimidazolium tetrafluoroborate ($EMImBF_4$) were synthesized according to literature methods [24,25].

2.2. Fabrication of dye-sensitized solar cells

Ionic liquid of HMImI and the binary ionic liquid mixture of HMImI and $EMImBF_4$ (weight ratio of 2:1) were mixed with 10 wt.% P(MOEMImCl), respectively, under vigorously stirring at 50 °C until they became transparent and stagnant. Lithium iodide (1 M) and iodine (0.5 M) were dissolved in the resulting self-standing gels to produce the quasi-state electrolytes. The

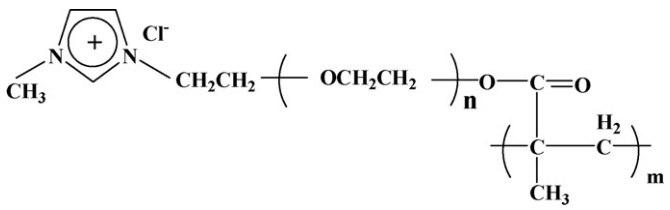

Scheme 1. Structure of the ionic liquid polymer P(MOEMImCl).

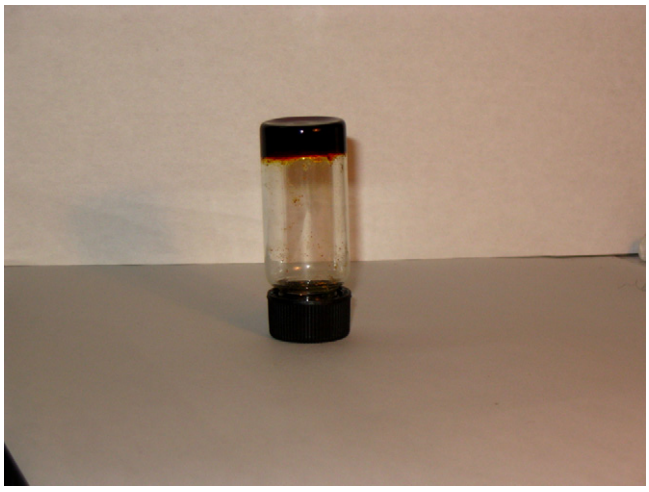

Fig. 1. Photography of ionic liquid based quasi-solid state electrolyte.

photograph of the prepared quasi-solid state electrolyte is given in Fig. 1.

TiO_2 colloidal paste was prepared and mixed with 10% monodispersed polystyrene spherical particles (200 nm in diameter) [26,27] under sonication. The prepared TiO_2 colloidal paste containing monodispersed polystyrene spherical particles was deposited on the transparent conductive glass sheets (FTO, 20 Ω/□) and then sintered at 450 °C for 30 min in air [26]. After removing the monodisperse polystyrene particles during the sintering, the nanocrystalline TiO_2 electrodes containing the larger size pores with the film thickness of 12 μm and the porosity of 60% were obtained. Incorporation of larger size pores into the nanocrystalline TiO_2 electrode aims at increasing the penetration of the gel electrolyte into the porous network and improving the interfacial contact between the TiO_2 nanoparticles and the electrolyte. Dye sensitization was performed by immersing the nanocrystalline TiO_2 electrodes in 5×10^{-4} M cis–bis (thiocyanato) bis(2,2′-bi-pyridyl-4,4′-dicarboxylate) ruthenium (II) ethanol solution overnight [26]. For fabrication of dye-sensitized solar cells, the quasi-solid state electrolytes were clamped in the gap between dye-sensitized nanocrystalline TiO_2 electrode as the photoanode and platinized conductive glass sheet as the counter electrode using a holder. Cell performance measurements were performed after placing the cell at the room temperature about 4 h for deeply penetrating the gel electrolyte and without any sealing.

2.3. Measurements

The ionic conductivities of quasi-solid state electrolytes were measured on Solartron 1225B frequency responser analyzer and Solartron SI 1287 electrochemical interface system. The sample was placed in a polytetrafluoroethylene ring which was clamped by two stainless electrodes. Stead-state voltammetry measurements were performed on PAR potentiostat (Model 273) at a scan rate of 50 mV s^{-1}. An electrochemical cell with a 10 μm radius Pt ultramicroelectrode as working electrode, Pt foil as counter electrode and Pt wire as reference electrode was used in the measurements [28]. Thermal stability was determined with

a thermogravimetric analyzer (Metch STA 409PC) over a temperature range of 35–700 °C at a heating rate of 10 °C min^{-1}. The test for evaporation of iodine was performed by placing the freshly prepared Electrolyte B (about 1 g) in a moisture analyzer with a air vent on the top (MB45, OHAUS), the evaporated iodine was detected by using the wet starch paper covered on the air vent of the analyzer.

Cross-sectional SEM images of the nanocrystalline TiO_2 electrodes were obtained on Scanning electron microscope (Hitachi-S-4300F). Two samples were prepared for the measurements. One sample was prepared by filling the nanocrystalline TiO_2 electrode with the gel electrolyte containing HMImI and 10 wt.% P(MOEMImCl) and clamping with a FTO glass substrate using a holder. Another sample was made by filling the nanocrystalline TiO_2 electrode with CH_3CCl_3 (1,1,1-trichloroethane) as a solvent saturating with P(MOEMImCl) solution and heating at 60 °C for about 2 h to penetrate the solution into the porous networks and to volatilize the solvent completely, then covering the surface with a FTO glass substrate. Both samples were placed in air at room temperature for about 4 h before the measurements. For the cell performance measurements, a 500 W xenon lamp with a 0.5 cm glass filter and a 10 cm water filter for cutting off the UV and IR irradiation was used as the light source. Photovoltaic performance was measured under the light intensity of 100 mW cm^{-2} detected by an optical power meter (Model 350) and a detector (Model 262) (UDT Instruments). The active area was 0.2 cm^2.

3. Results and discussion

Ionic liquid based quasi-solid state electrolytes containing 1 M lithium iodide and 0.5 M iodine were successfully prepared by solidifying the ionic liquid HMImI or the binary ionic liquid mixture of HMImI and $EMImBF_4$ (weight ratio of 2:1) with 10 wt.% of P(MOEMImCl) to produce Electrolyte A and Electrolyte B, respectively. HMImI employed as the important iodide source in both electrolytes has a higher viscosity of 1800 mPa s. Incorporating $EMImBF_4$ having a lower viscosity of 37 mPa s (25 °C) [25] into Electrolyte B enables decrease of the viscosity [9]. Both quasi-solid state electrolytes exhibit the high ionic conductivities comparable to that of the liquid electrolytes.

The penetration of the gel electrolyte was examined by the cross-sectional SEM images of nanocrystalline TiO_2 electrode shown in Fig. 2. Fig. 2a is the cross-sectional SEM image of nanocrystalline TiO_2 electrode with the large size pores. From Fig. 2b it is observed that the TiO_2 nanoparticles are covered with the gel electrolyte containing HMImI and 10 wt.% P(MOEMImCl) and the shape of nanoparticles cannot be distinguished in the image confirming the efficient penetration of the gel electrolyte into the nanopores. In order to clarify the penetration of gel electrolyte containing HMImI and P(MOEMImCl) rather than HMImI alone. The penetration of the P(MOEMImCl) is further explored in Fig. 2c. An apparent increase in the size of the nanoparticles indicates that the surface is coated with P(MOEMImCl). P(MOEMImCl) dissolved in CH_3CCl_3 solvent can penetrate into the nanopores and subse-

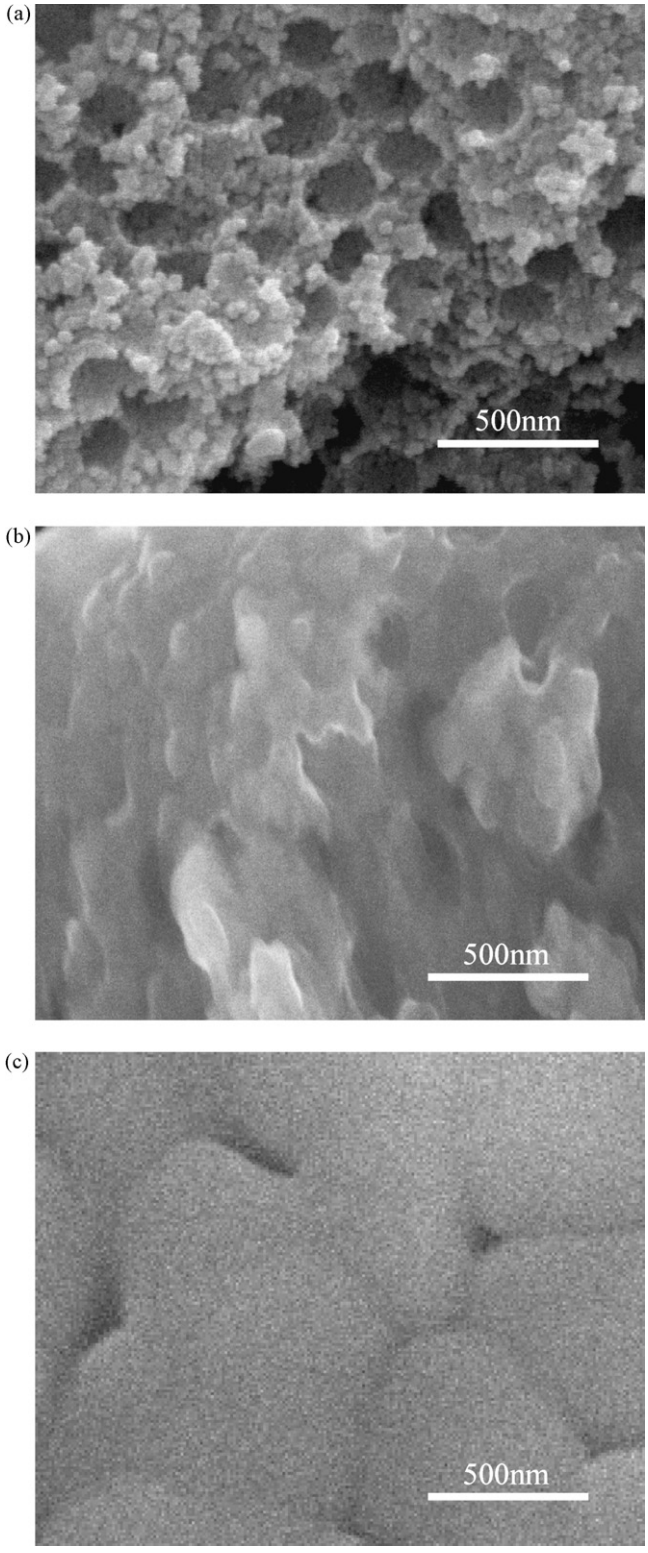

Fig. 2. Cross-sectional SEM images of the nanocrystalline TiO_2 electrode: (a) before filling, (b) after filling with the gel electrolyte containing HMImI and 10 wt.% P(MOEMImCl) and (c) after filling with the ionic liquid polymer of P(MOEMImCl).

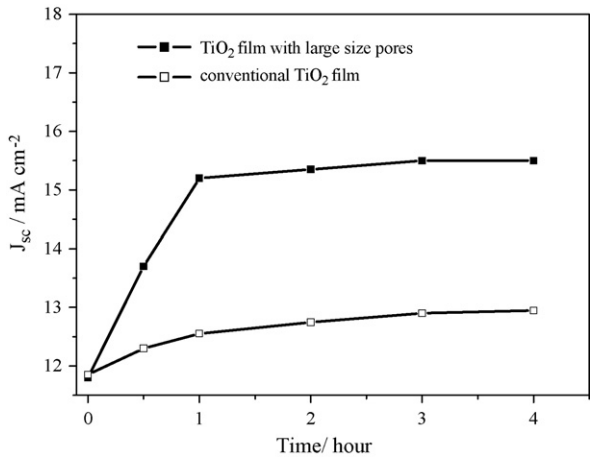

Fig. 3. Short-circuit photocurrent density of DSSCs as a function of the penetration time of Electrolyte B. The porosities of 60% for the nanocrystalline TiO_2 electrode with larger size pores and 55% for the conventional TiO_2 nanocrystalline TiO_2 electrode.

quently deposited on the nanoparticles after volatilization of the solvent. The improvement of the contact between the gel electrolyte and the nanoparticles was further revealed by measuring the short-circuit photocurrent J_{sc} of DSSCs as a function of the penetration time of Electrolyte B. The data on the DSSCs with the conventional nanocrystalline TiO_2 electrode is illustrated for comparison. As shown in Fig. 3, J_{sc} increases initially and trends to a saturation after 1 h for both cases. The large J_{sc} obtained for the nanocrystalline TiO_2 electrode containing larger size pores compared to that of the conventional nanocrystalline TiO_2 electrode indicates the improvement of the interfacial contact due to increasing the penetration of Electrolyte B into the porous networks.

Ionic conductivity and ionic diffusion coefficient of the electrolytes are the important parameters that significantly influence the cell performance of the quasi-solid state dye-sensitized solar cells. Fig. 4 shows the dependence of the ionic conductivity on the polymer content of the gel electrolytes. It is found that the

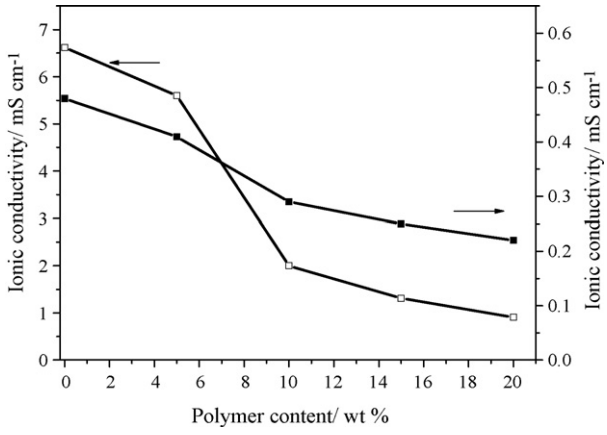

Fig. 4. Dependence of the ionic conductivity of electrolytes on the polymer content. Open square: 0.5 M lithium iodide, 0.05 M iodine in ionic liquid of HMImI, filled square: 0.5 M lithium iodide, 0.05 M iodine in the binaryionic liquid mixture of HMImI and $EMImBF_4$. The ionic conductivity was measured at 25 °C.

ionic conductivity decreases with increasing the polymer content for both gel electrolytes. The ionic conductivity in the gel electrolyte with the binary ionic liquid mixture of HMImI and $EMImBF_4$ is significantly higher than that in the gel electrolyte with the HMImI at various polymer content. The ionic conductivity of 2.0×10^{-3} S cm^{-1} obtained at the polymer content of 10 wt.% for the gel electrolyte with the binary ionic liquid mixture of HMImI and $EMImBF_4$ (Electrolyte B) is about 1 order of magnitude higher than the value of 2.9×10^{-4} S cm^{-1} obtained in the gel electrolyte with ionic liquid HMImI at the same polymer content (Electrolyte A). The observed dependence of the ionic conductivity on the polymer content and ionic liquid in the gel electrolytes is related to the viscosity of the gel electrolytes. According to the Stokes–Einstein equation $D = kT/6\pi\eta_e r$, the product of the diffusion coefficient and viscosity ($D\eta_e$) is approximately constant for the diffusing species having the unchangeably effective ion radius (r) in the electrolytes of various viscosities at a given temperature [9]. From the product of $D\eta_e$, it can be analyzed that an increase of η_e in the gel electrolyte with higher polymer content results in the decrease of D. Since D is directly proportional to the ionic mobility and therefore the ionic conductivity, thus, the ionic conductivity decreases in the gel electrolyte with higher polymer content where the viscosity increases. Based on the Stokes-Einstein equation, A decrease of viscosity in the gel electrolyte of binary ionic liquid mixture of HMImI and $EMImBF_4$ with respect to that in the gel electrolyte of ionic liquid HMImI due to the contribution of $EMImBF_4$ which has lower viscosity of 37 mPa s (25 °C) [25] leads to the higher ionic conductivity obtained in Electrolyte B than that in Electrolyte A.

The stead-state voltammograms for the reduction of I_3^- in the Electrolyte A and Electrolyte B are depicted in Fig. 5. From the cathodic stead-state currents (I_{ss}), the apparent diffusion coef-

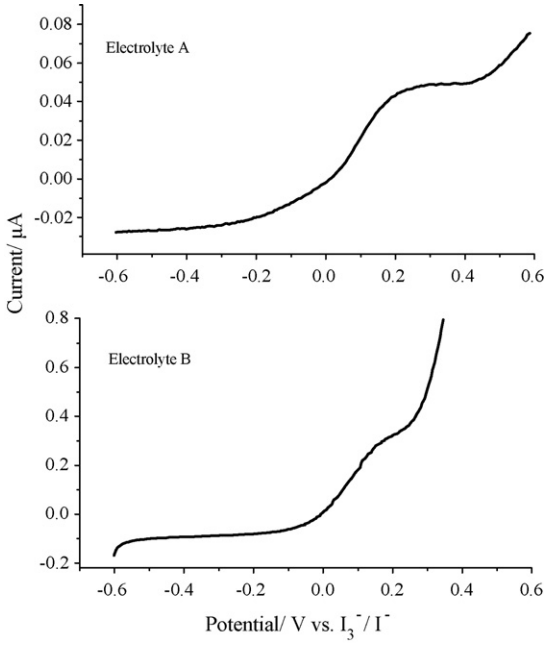

Fig. 5. Steady-state voltammograms for the Pt ultramicroelectrode in Electrolyte A and Electrolyte B. Scan rate: 50 mV s^{-1}.

Table 1
The apparent diffusion coefficient of I_3^- and the diffusion limiting current density

Electrolyte	$D_{app}(I_3^-)$, $cm^2\ s^{-1}$	J_{lim}, $mA\ cm^{-2}$
Electrolyte A	6.66×10^{-8}	9.6
Electrolyte B	2.13×10^{-7}	30.8

ficients (D_{app}) of I_3^- can be calculated by using the following equation [28].

$$I_{ss} = 4nCaFD_{app} \quad (1)$$

where n is the electron transfer number per molecule, C the initial concentration of electroactive species, a the radius of the Pt ultramicroelectrode and F is the Faraday constant. As shown in Table 1, the calculated apparent diffusion coefficient of I_3^- in Electrolyte B is about three times larger than that in Electrolyte A. It has been known that the Grotthus type electron exchange between triiodide and iodide makes a significant contribution to the apparent diffusion coefficient of I_3^- in the ionic liquid based gel electrolytes [16,17]. However, the larger apparent diffusion coefficient of I_3^- in Electrolyte B is suggested to reflect the contribution from the physical diffusion of triiodide due to the lower viscosity of this gel electrolyte [10].

From the apparent diffusion coefficient of I_3^-, the diffusion limiting current density (J_{lim}) can be calculated in terms of Eq. (2) [13]:

$$J_{lim} = 6\varepsilon FD_{app}(I_3^-)\frac{C(I_3^-)}{L} \quad (2)$$

where ε is the porosity of the TiO_2 film, $C(I_3^-)$ the initial concentration of I_3^- and L is the film thickness. Due to the excess iodide in the electrolyte, the diffusion of triiodide can be an important factor that limits the overall photocurrent density current density of the cell especially at high light intensity irradiation. If the diffusion limiting current density is smaller than the photocurrent density delivered from the nanocrystalline TiO_2 electrode, the overall photocurrent density current density of the nanocrystalline cell will be limited by the diffusion of I_3^- in the electrolyte. The calculated diffusion limiting current densities for both electrolytes are given in Table 1. It is observed that the J_{lim} of Electrolyte B is significantly larger than that of Electrolyte A. The larger J_{lim} of Electrolyte B is advantageous to decrease the losses of overall photocurrent density of the nanocrystalline cell. The dependence of J_{sc} on the incident light intensity shown in Fig. 6 provides the information of mass transport limitation in both electrolytes. The short-circuit photocurrent density obtained in the nanocrystalline cell containing Electrolyte A increases with the light intensity until $60\ mW\ cm^{-2}$ and trends to a saturation at the light intensities $>60\ mW\ cm^{-2}$ indicating the limitation of the J_{sc} at high light intensity. In the case of the nanocrystalline cell containing Electrolyte B, the short-circuit photocurrent density increases proportionally with the light intensity up to $100\ mW\ cm^{-2}$. These results imply that the J_{sc} is not limited by the diffusion of I_3^- in the Electrolyte B until the light intensity of $100\ mW\ cm^{-2}$ due to the large diffusion limiting current density.

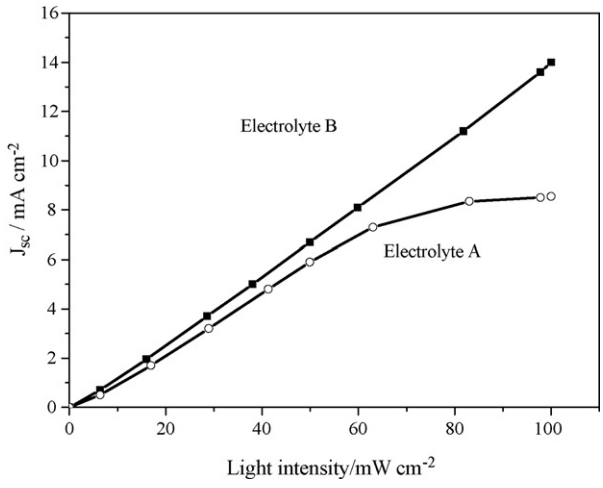

Fig. 6. Dependence of the short-circuit photocurrent density on the light intensity for DSSCs with Electrolyte A and Electrolyte B.

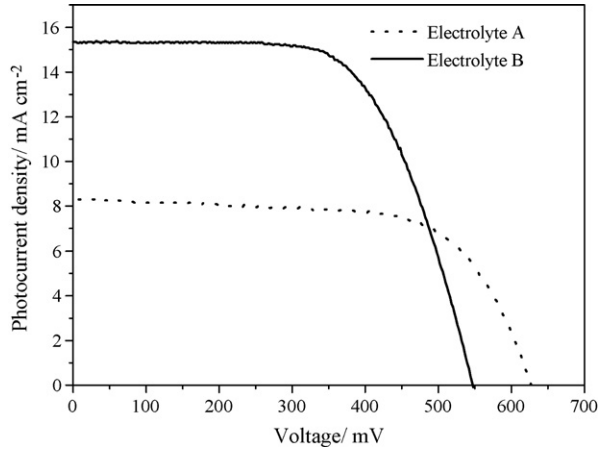

Fig. 7. Photocurrent density–voltage curves for DSSCs with Electrolyte A and Electrolyte B.

The photocurrent density (J)–voltage (V) curves of the quasi-solid state DSSCs is illustrated in Fig. 7. The Photovoltaic parameters including the short circuit photocurrent density (J_{sc}), open circuit voltage (V_{oc}), fill factor (FF) and conversion efficiency (η) obtained from the J–V curves are summarized in Table 2. The pronounced increase of the J_{sc} is observed in the nanocrystalline cell with Electrolyte B resulting in the conversion efficiency of 5.3% which is higher than that with Electrolyte A. Further improvement of the V_{oc} is achieved in the nanocrystalline cell with Electrolyte B by adding *N*-methybenzimidazole (NMBI) to the electrolyte. Fig. 8 shows the J–V curve and the photovoltaic parameters of the nanocrystalline cell with the Electrolyte B containing 0.5 M NMBI. The open circuit volt-

Table 2
Photovoltaic performance of DSSCs with Electrolytes A, B

Electrolyte	J_{sc}, $mA\ cm^{-2}$	V_{oc}, mV	FF	η, %
Electrolyte A	8.30	626	0.67	3.5
Electrolyte B	15.35	546	0.64	5.3
Electrolyte B[a]	15.50	618	0.64	6.1

[a] Containing 0.5 M NMBI.

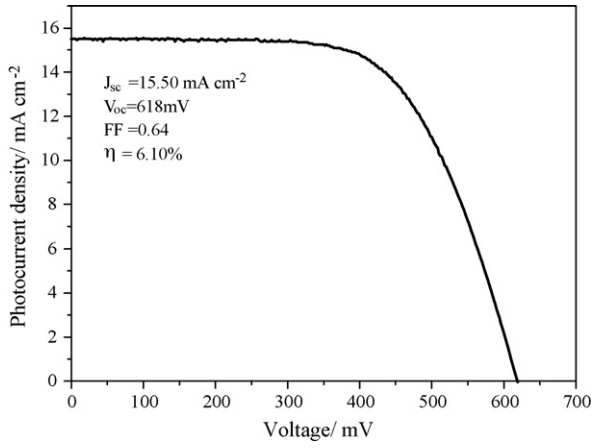

Fig. 8. Photocurrent density–voltage curve for DSSCs with Electrolyte B containing 0.5 M NMBI.

age increases by 72 mV yielding the conversion efficiency of 6.1%. NMBI used as the non-volatile additive in the electrolyte has the strong effect on improving the V_{oc} that was revealed in the previous work [29]. Since the flat-band potentials of TiO_2 electrode measured in the Electrolyte B with and without NMBI are almost the same value (−0.80 V versus SCE). The increase of V_{oc} is rationalized in terms of the adsorption NMBI on the TiO_2 surface, which suppresses the surface recombination via passivation of the surface states rather than shifts the flat-band potential of TiO_2 electrode.

The thermal stability of the Electrolyte B was examined by the thermogravimetric analysis. Fig. 9 depicts the thermogravimetric curve of the Electrolyte B. The loss in weight occurred at the temperature higher than 200 °C whereas it was negligible at the temperature lower than 200 °C. From the thermogravimetric curve, it is evaluated that the loss in weight about 7% occurred in the temperature range of 200–300 °C and about 90% took place in 300–500 °C. The negligible loss in weight at the temperature ≤200 °C indicates the excellent thermal stability of the Electrolyte B. This is the most desirable properties for fabrication of the quasi-solid state DSSCs with high efficiency and long term stability.

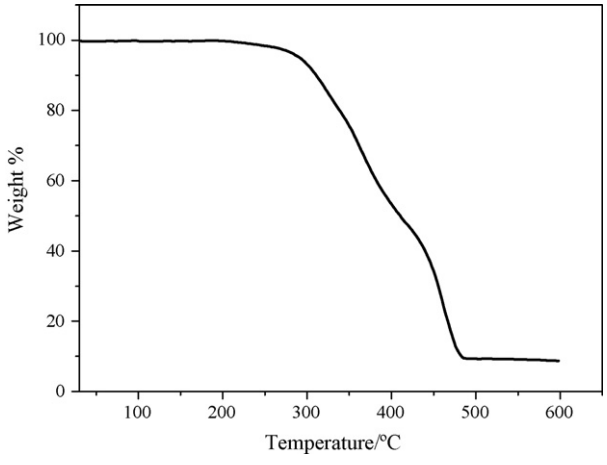

Fig. 9. Thermal gravimetric analysis of Electrolyte B.

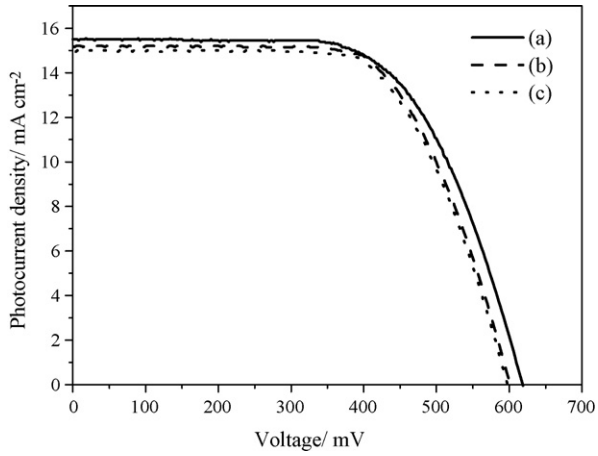

Fig. 10. Photocurrent density–voltage curves for DSSCs with Electrolyte B measured (a) at 30 °C for 5 min (b) after heat treatment at 100 °C for 30 min (c) after heat treatment at 100 °C for 120 min.

Table 3
Effect of heat treatments on the photovoltaic performance of DSSCs with Electrolyte B

Heat treatments	J_{sc}, mA cm^{-2}	V_{oc}, mV	FF	η, %
(a) 30 °C for 5 min	15.50	618	0.64	6.10
(b) 100 °C for 30 min	15.20	598	0.66	5.97
(c) 100 °C for another 120 min	15.00	594	0.66	5.86

The influence of heat-treatments on the photovoltaic performance of the nanocrystalline cell with Electrolyte B is illustrated in Fig. 10 and Table 3. It is found that heat-treatments result in a decrease of cell performance. The decreases in the conversion efficiency about 2.1 and 3.9% after heat- treatments at 100 °C for 30 and 120 min, respectively, are evaluated from the data listed in Table 3. The degradation occurs during heat-treatment resulting from the evaporation of iodine at elevated-temperature [30]. This is confirmed by detecting the evaporated iodine during the heat-treatment at 100 °C in an analyzer using a wet starch paper. Additional, it is speculated that the dye desorption could also be the cause of the decrease in cell performance at elevated-temperature. Since dye adsorption on the TiO_2 surface is in equilibrium with dye desorption and this adsorption/desorption equilibrium shifts depending on the temperature [31].

4. Conclusions

P(MOEMImCl) as the ionic liquid polymer was synthesized and used to solidify the ionic liquid electrolytes for fabrication of quasi-solid state dye-sensitized solar cells. The ionic liquid based quasi-solid state electrolytes containing 1 M lithium iodide and 0.5 M iodine in the ionic liquid of HMImI or the binary ionic liquid mixture of HMImI and $EMImBF_4$ (weight ratio of 2:1), respectively, were prepared with 10 wt.% P(MOEMImCl). The higher ionic conductivity and larger apparent diffusion coefficient of triiodide are exhibited in the binary ionic liquid mixture gel electrolyte. The negligible loss in weight at the temperature ≤200 °C for Electrolyte B was determined by thermogravimetric analysis confirming the excellent thermal

stability. A conversion efficiency of 6.1% under the irradiation of 100 mW cm^{-2} was achieved for the quasi-solid state DSSCs containing the binary ionic liquid mixture gel electrolyte. The effect of the heat-treatments on the cell performance was studied indicating the drops in conversion efficiency about 2.1 and 3.9% after heat treatments at 100 °C for 30 and 120 min, respectively.

Acknowledgments

The authors thank the financial supports provided by National Research Fund for Fundamental Key Project (2006CB202605), High-Tech Research and Development of China Program (2002AA302403) and National Natural Science Foundation of China (20373075, 50221201 and 50473055).

References

[1] A. Hagfeldt, M. Grätzel, Chem. Rev. 95 (1995) 49–68.
[2] B. O′.Regan, M. Grätzel, Nature 353 (1991) 737–739.
[3] M. Grätzel, Nature 414 (2001) 338–344.
[4] A.F. Nogueria, J.R. Durrant, M.A. Depaoli, Adv. Mater. 13 (2001) 826–830.
[5] A.F. Nogueria, M.A. Depaoli, I. Montanari, R. Monkhouse, J. Nelson, J.R. Durrant, J. Phys. Chem. B 105 (2001) 7517–7524.
[6] T. Stergiopoulos, I.M. Arabatzis, G. Katsaros, P. Falaras, Nano Lett. 2 (2002) 1259–1261.
[7] G. Katsaros, T. Stergiopoulos, I.M. Arabatzis, K.G. Papadokostaki, J. Photochem. Photobiol. A: Chem. 149 (2002) 191–198.
[8] P. Wang, S.M. Zakeeruddin, M. Grätzel, J. Fluorine Chem. 125 (2004) 1241–1245.
[9] N. Papageorgiou, Y. Athanassov, M. Armand, P. Bonhôte, H. Pettersson, A. Azam, M. Grätzel, J. Electrochem. Soc. 143 (1996) 3099–3108.
[10] P. Wang, S.M. Zakeeruddin, R.H. Baker, M. Grätzel, Chem. Mater. 16 (2004) 2694–2696.
[11] P. Wang, S.M. Zakeeruddin, J.E. Moser, M. Grätzel, J. Phys. Chem. B 107 (2003) 13280–13285.
[12] W. Kubo, Y. Makimoto, T. Kitamura, Y. Wada, S. Yanagida, Chem. Lett. (2002) 948–949.
[13] W. Kubo, S. Kambe, S. Nakade, T. Kitamura, K. Hanabusa, Y. Wada, S. Yanagida, J. Phys. Chem. B 107 (2003) 4374–4381.
[14] P. Wang, S.M. Zakeeruddin, J.-E. Moser, R.H. Baker, M. Grätzel, J. Am. Chem. Soc. 126 (2004) 7164–7165.
[15] P. Wang, B. Wenger, R.H. Baker, J.-E. Moser, J. Teuscher, W. Kantlehner, J. Mezger, E.V. Stoyanov, S.M. Zakeeruddin, M. Grätzel, J. Am. Chem. Soc. 127 (2005) 6850–6856.
[16] P. Wang, S.M. Zakeeruddin, I. Exnar, M. Grätzel, Chem. Commun. (2002) 2972–2973.
[17] P. Wang, S.M. Zakeeruddin, P. Comte, I. Exnar, M. Grätzel, J. Am. Chem. Soc. 125 (2003) 1166–1167.
[18] H. Ohno, Electrochim. Acta 46 (2001) 1407–1411.
[19] M. Yoshizawa, H. Ohno, Chem. Lett. (1999) 889–890.
[20] M. Yshizawa, H. Ohno, Electrochim. Acta 46 (2001) 1723–1728.
[21] S. Zalipsky, C. Gilon, A. Zilkha, Eur. Polym. J. 19 (1983) 1177–1183.
[22] Y. Nakai, K. Ito, H. Ohno, Solid State Ionics 113–115 (1998) 199–204.
[23] S. Washiro, M. Yashizawa, H. Nakajima, H. Ohno, Polymer 45 (2004) 1577–1582.
[24] W. Kubo, T. Kitamura, K. Hanabuse, Y. Wada, S. Yanagida, Chem. Commun. (2002) 374–375.
[25] T. Nishida, Y. Tashiro, M. Yamamoto, J. Fluorine Chem. 120 (2003) 135–141.
[26] G. Wang, X. Zhou, M. Li, J. Zhang, J. Kang, Y. Lin, S. Fang, X. Xiao, Mater. Res. Bull. 39 (2004) 2113–2118.
[27] Z.Z. Yang, D. Li, J.H. Rong, W.D. Yan, Z.W. Niu, Macromol. Mater. Eng. 287 (2002) 627–633.
[28] B.M. Quinn, Z. Ding, R. Moulton, A.J. Bard, Langmuir 18 (2002) 1734–1742.
[29] E. Stathatos, P. Lianos, S.M. Zakeeruddin, P. Liska, M. Grätzel, Chem. Mater. 15 (2003) 1825–1829.
[30] K. Suzuki, M. Yamaguchi, S. Hotta, N. Tanabe, S. Yanagida, J. Photochem. Photobiol. A: Chem. 164 (2004) 81–85.
[31] P.M. Sommeling, M. Späth, H.J.P. Smit, N.J. Bakker, J.M. Kroon, J. Photochem. Photobiol. A: Chem. 164 (2004) 137–144.